Published in final edited form as:
ACS Nano. 2013 August 27; 7(8): 6667–6673. doi:10.1021/nn402753y.

Direct Delivery of Functional Proteins and Enzymes to the Cytosol Using Nanoparticle-Stabilized Nanocapsules

Rui Tang, **Chang Soo Kim**, **David J. Solfiell**, **Subinoy Rana**, **Rubul Mout**, **Elih M. Velázquez-Delgado**, **Apiwat Chompoosor**, **Youngdo Jeong**, **Bo Yan**, **Zheng-Jiang Zhu**, **Chaekyu Kim**, **Jeanne A. Hardy**, and **Vincent M. Rotello***
Department of Chemistry, University of Massachusetts-Amherst, 710 North Pleasant Street, Amherst, Massachusetts, 01003, USA

Abstract

Intracellular protein delivery is an important tool for both therapeutic and fundamental applications. Effective protein delivery faces two major challenges: efficient cellular uptake and avoiding endosomal sequestration. We report here a general strategy for direct delivery of functional proteins to the cytosol using nanoparticle-stabilized capsules (NPSCs). These NPSCs are formed and stabilized through supramolecular interactions between the nanoparticle, the protein cargo, and the fatty acid capsule interior. The NPSCs are ~130 nm in diameter and feature low toxicity and excellent stability in serum. The effectiveness of these NPSCs as therapeutic protein carriers was demonstrated through the delivery of fully functional caspase-3 to HeLa cells with concomitant apoptosis. Analogous delivery of green fluorescent protein (GFP) confirmed cytosolic delivery as well as intracellular targeting of the delivered protein, demonstrating the utility of the system for both therapeutic and imaging applications.

Keywords

nanoparticle; nanocapsule; intracellular protein delivery; supramolecular assembly; organelle targeting

Protein-based therapeutics are promising tools for numerous biomedical applications.[1] Intracellular delivery of functional proteins to replace missing, dysfunctional or poorly-expressed proteins, or antagonize key intracellular pathways is the fastest growing and a promising arm in modern drug development. Protein-based biologics have provided new therapeutic avenues for cancer,[2,3] and have also been used to treat a range of disease states including inflammation,[4] lysosomal storage diseases,[5] and transient cerebrovascular disorders.[6] In addition to therapeutics, direct cytosolic delivery of functional proteins provides a potential tool for important biological applications including imaging,[7] signaling studies,[8,9] cellular[10, 11] and stem cell engineering.[12]

A major complication in the use of protein-based drugs is the difficulty of delivering the unmodified, functional protein in an active conformation to the necessary site of action.

*Address correspondence to rotello@chem.umass.edu..

Conflicts of Interest: The authors declare no competing financial interests.

Supporting Information Available: Additional experimental details and figures. This material is available free of charge *via* the Internet at http://pubs.acs.org.

Contributions. RT, DJS, AC, and VMR conceived and designed the experiments. RT, DJS, SR, CSK, ZJZ, CK, RM, BY, EMV and YJ performed the experiments. All authors analyzed and discussed the data. RT wrote the manuscript, with revisions by DJS, CSK, SR, JAH and VMR.

Mechanical delivery methods, such as microinjection and electroporation have been used in research for decades.[13] These methods, however, are low-throughput, disruptive, and require specialized equipments to mechanically/physically puncture membranes, limiting their utility for *in vivo* applications. Another promising approach for delivering proteins utilizes covalent carriers[14,15] that require irreversible modifications of the protein cargo.[16,17] However, these covalent modifications of protein may impact protein function by interfering with protein folding.[18, 19] Furthermore, covalent modification of proteins for delivery is not a general approach; in cases where this strategy works customized optimization protocols tailored to each specific protein are required.[14]

A major challenge in all the non-mechanical protein delivery strategies described above is access of the protein to the cytosol. Most delivery strategies rely on endocytic mechanisms of cellular uptake.[20] As a result, the delivered proteins are susceptible to degradation in the endosome/lysosome and are also unable to access key subcellular structures and machineries required for most applications.[15] Currently, prolonged incubation times, elevated concentrations of delivery agents, and lysosomotropic reagents (such as chloroquine) are required to increase the efficiency of endosomal escape of delivered proteins.[21,22]

Supramolecular carrier-based delivery methods are modular, easy to formulate, and operate through reversible associations with target proteins.[23] In non-covalent strategies, proteins and delivery vectors self-assemble, allowing the transport of unmodified proteins into the cell and overcome the limitations of using covalently protein modification strategies.[14,15]

We have recently developed a nanoparticle-stabilized capsule (NPSC) system for the delivery of hydrophobic drugs.[24] These NPSCs rapidly released small molecule payloads from their oil interior through a membrane fusion-like[25, 26] hydrophobic interaction with the cell membrane. We hypothesized that this vehicle could also be used for cytosolic protein delivery by incorporating functional proteins into the NPSC shell. In this report, we demonstrate rapid and efficient delivery of therapeutic and imaging proteins into the cytosol of HeLa cells using NPSCs. Caspase-3 (CASP3) was chosen to demonstrate therapeutic delivery of an active, biomedically important enzyme. Delivery of CASP3 is a particularly stringent test of the efficacy of this approach, as caspases are delicate enzymes that would be susceptible to inactivation during the delivery process. CASP3 was efficiently delivered into cells, resulting in effective induction of apoptosis. Green fluorescent protein (GFP) was used to determine the intracellular distribution of delivered proteins. The delivered GFP was distributed throughout the cell with identical cellular distribution to that of endogenously expressed red fluorescent protein (RFP). Further proof of cytosolic access was demonstrated through efficient intracellular targeting of a GFP fusion protein to the peroxisome.[27]

RESULTS AND DISCUSSION

Nanoparticle-stabilized capsule fabrication

The protein-NPSC (CASP3-NPSC and GFP-NPSC) complexes were generated using a convergent process (Figure 1a, see Methods), where the HKRK AuNPs (see Figure 1a for the structure) provided a dual mode supramolecular stabilization of the capsule wall. Briefly, proteins and AuNPs were mixed and incubated at room temperature for 10 minutes. Template emulsions were formed by homogenizing AuNPs in phosphate buffer (5 mM, pH 7.4) and oil. Protein-NPSCs were formed by combining template emulsions and the protein-AuNP mixture. Combined hydrogen bonding and electrostatic interactions between the guanidinium moieties of the particles and the carboxylates of the oil[28,29] pin the nanoparticles to the capsule surface. Lateral stabilization is provided through interactions of the cationic nanoparticles with the anionic proteins (GFP pI= 5.9, CASP3 pI= 6.1) to be transported (Figure 1a).[30] The capsule size is well-controlled and in a regime well suited for

intracellular delivery[31] with GFP-NPSCs and CASP3-NPSCs possessing average diameters as determined by dynamic light scattering of 130 ± 40 nm and 140 ± 20 nm, respectively (Figure 1b and c, Figure S1).

A fluorescence titration was performed to measure the binding constant (K_s) between HKRK AuNPs and GFP, which was found to be 9×10^7 M^{-1}, indicating high affinity of HKRK AuNPs to the protein (Figure S2a). Screening of the electrostatic interactions through the use of 500 mM NaCl into the mixture of AuNPs with GFP at 1:1 molar ratio resulted in complete recovery of the GFP fluorescence (Figure S2b), indicating reversible electrostatic interactions between the HKRK AuNP and the protein. GFP is almost completely quenched upon complexation by AuNPs. NPSC formation, however, results in a partial restoration in fluorescence. This result indicates a change in the structure of GFP-AuNP complex when at the interface of the NPSCs. To further probe the nature of the interactions, the NPSCs were incubated in 0.5% Tween-20 and 500 mM NaCl solutions. The high salt solution resulted in no change in fluorescence, while Tween-20 resulted in increased in fluorescence. (79%; Figure S3). These results suggest that other interactions are involved in NPSC assembly beyond simple electrostatics. For CASP3, enzyme activity was assessed after interaction with HKRK AuNPs. Activity assays *in vitro* showed that the interaction between CASP3 and HKRK AuNPs did not inhibit the enzymatic activity. In fact, HKRK AuNPs enhanced the CASP3 activity by 2.3 times, a phenomenon observed previously in other nanoparticle-protein systems[32] (Figure S4). While efforts were made to assess activity of CASP3 in the NPSCS, the biphasic nature of the system prevented effective measurement of catalytic efficiency.

Therapeutic protein delivery with NPSCs

Effective use of therapeutic proteins for intracellular applications requires rapid delivery of the protein in the active form to the cytosol.[33, 34] CASP3 is a highly promising therapeutic protein candidate[35] owing to its critical role in apoptosis.[36] Most tumor cells do not undergo appropriate apoptosis, which leads to unhindered cell growth.[37] In many tumor cells CASP3 function is blocked due to over expression of inhibitor of apoptosis (IAP) proteins that directly inhibit caspase function preventing apoptosis. Intracellular delivery of sufficient levels of active CASP3 into the cytosol of such tumor cells circumvents this blockage, allowing tumor cells to enter apoptosis. Delivery of active caspases is extremely challenging, however, due to the negative charge and heterotertrameric state of the protein, the susceptibility of the active site to oxidation and alkylation, and the fragile nature of the active site that is composed of four highly mobile loops.

Demonstration of effective delivery of active CASP3 was established through incubation of HeLa cells with CASP3-NPSCs. After 1 h incubation, 72.0 ± 5.5% of HeLa cells underwent apoptosis, confirmed by double staining with Yopro-1 (a dye to detect apoptotic cell nuclei)[38] and 7-AAD (a dye used to detect membrane disruption)[39] (Figure 2a). The NPSC itself (Figure 2b), CASP3 only (Figure 2c), or CASP3 with AuNPs (Figure S5d) induced minimal levels of cell apoptosis, demonstrating that CASP3-NPSCs deliver the protein in the active form required for therapeutic applications.

GFP delivery using NPSCs

The effectiveness of the delivered caspase suggested access of the delivered protein to the cytosol. The capability of cytosolic delivery of NPSCs was verified using GFP. Imaging experiments were performed using live cells to provide an accurate determination of protein distribution inside the cell.[40] After 1 h incubation of GFP-NPSCs with HeLa cells, followed by 1 h incubation in fresh media, GFP was observed evenly distributed throughout the cytosol and nucleus (Figure 3a). In comparison, no delivery was observed by mixing empty

NPSCs and GFP, indicating that the NPSCs serve as a carrier for the delivery cargo and not solely as a "hole puncher" for membrane penetration (Figure S6). To further demonstrate the cytosolic distribution of GFP, NPSCs were used to deliver GFP into mCherry expressing HeLa cells.[41] Confocal images (Figure 3b and Figure S7) show GFP delivered *via* NPSCs to be evenly distributed throughout the cytosol and nucleus (with the exception of nucleoli) of HeLa cells, with no perceptible difference in distribution with respect to mCherry. Co-administration of Hoechst 33342 (a family of blue fluorescent dyes used to stain nuclei) confirmed that the delivered GFP had gained access to the nucleus, but not to the interiors of nucleoli (Figure S6), consistent with the distribution of cellularly expressed mCherry. Dispersal of GFP in the nucleus indicated that GFP was successfully delivered not just to the cytosol, but also to the nucleus by free diffusion through nuclear pores.[42] Taken together, these results demonstrate that the GFP was successfully delivered into the cytosol in a freely diffusing fashion.

Flow cytometry was used to quantify the efficiency of GFP delivery into cells using NPSCs. The results showed that GFP was delivered to 77 ± 5% of cells in the GFP-NPSCs group (Figure 3c), consistent with the apoptosis induction observed with the CASP3-NPSCs. As expected, no delivery was observed for either the cells treated with GFP alone or untreated. Only low levels of delivery (20.6 ± 3.8%) were observed for GFP-HKRK AuNP complexes that were not in capsule form (Figure S9), with most of the delivered GFP remaining entrapped in late endosomes/lysosomes (Figure S10). The difference in GFP delivery efficiency and subcellular localization between the particle-only group and the NPSC group supports the hypothesis that the improved efficiency of the delivery process in the NPSC group resulted from a membrane fusion-delivery process, in agreement with previous studies.[24,43,44] The NPSCs showed little cytotoxicity at the concentration (29 pM) used for the delivery studies (Figure S11).

Live cell video imaging was then performed to track the intracellular release of protein payloads by NPSCs (Figure 4 and Movies S1, S2). As shown in Figure 4 and Movie S1, GFP-NPSCs remain intact for the first few minutes after attaching to the cell, confirmed by the colocalization of GFP and the AuNPs. Then GFP was rapidly released into cytosol within. As seen from Movie S2, GFP was rapidly delivered, however the GFP-NPSC was not taken up as an intact entity by the cell. Taken together, these results strongly support the membrane fusion mechanism of delivery while demonstrating that uptake does not occur through an endocytotic mechanism

Intracellular targeting of delivered proteins

To further demonstrate the versatility of NPSC protein delivery for intracellular delivery and imaging, we fused a peroxisomal-targeting sequence 1 (PTS1) to GFP (Figure S12).[45] HeLa cells with stable expression of RFP bearing a C-terminal peroxisomal-targeting sequence were used to provide a fluorescence label for the peroxisomes. After 1 h incubation with GFP-PTS1-NPSC complexes, followed by 1 h incubation with fresh media, the confocal images clearly confirmed complete colocalization of the GFP-PTS1 fusion protein with the RFP-labeled peroxisomes (Figure 5a and Figure S13). In contrast, GFP without the PTS1 motif was evenly distributed throughout the cell as previously described (Figure 5b). These results clearly demonstrate that the protein delivered by the NPSCs gained complete access to the cytosol, and that proteins delivered by NPSCs are capable of targeting subcellular organelles with essentially identical localization behavior to cellularly expressed proteins.[27]

CONCLUSION

We have demonstrated a rapid and efficient protein delivery strategy using nanoparticle based supramolecular nanocapsules. This approach provides a generalized strategy for direct

delivery of functional proteins in their native forms. The supramolecular structure of the NPSCs makes the system stable for delivery of proteins yet reversible for payload release. In contrast with particle based protein delivery systems, this method is capable of overcoming the major challenge of endosomal sequestration and thus holds great promise for effective protein therapy and imaging applications. We demonstrated the efficiency of the system by delivering a functional therapeutic protein, CASP3 into target cells to induce apoptosis. Delivery of fluorescent proteins demonstrated cytosolic distribution identical to that of a cellularly expressed counterpart, with delivery versatility further demonstrated by subcellular targeting of proteins. Taken together, the ability to incorporate active proteins on the capsule shell and efficiently deliver into the cytosol opens up new opportunities for protein replacement therapy, *in vivo* disease prognosis through imaging, cellular organelle labeling, and cellular engineering.

METHODS

Protein-NPSC complex preparation

The HKRK ligand protected AuNPs (HKRK AuNPs) were synthesized following reported method.[30] To make the protein-NPSC complex, 2.5 μM HKRK AuNPs were incubated with 1 μM GFP in 30 μL phosphate buffer (5 mM, pH = 7.4) for 10 min. Then, 1 μL of the mixture of linoleic acid and decanoic acid (molar ratio = 1:1) was mixed with 500 μL of phosphate buffer (5 mM, pH = 7.4) containing 1 μM HKRK AuNPs and agitated by an amalgamator at 5000 rpm for 100 s to form emulsions. Finally, the mixture of the protein and HKRK AuNPs was diluted to 45 μL with phosphate buffer (5 mM, pH = 7.4) followed by the addition of 5 μL of the emulsion. The protein-NPSC complexes were ready to use after 10 min incubation at room temperature. The concentration of NPSC was 0.29 nM, calculated according to reported method.[24] The final concentrations of HKRK AuNPs and GFP were 1.5 μM and 600 nM, respectively.

GFP delivery

60,000 or 240,000 HeLa cells or transfected HeLa cells were cultured in a 24-well plate or confocal dish, respectively, for 24 h prior to delivery. The cells were washed by cold phosphate buffer saline (PBS) 3 times right before delivery. After the preparation of cells, GFP-NPSC complex solution (50 μL or 150 μL of the GFP-NPSC complex diluted by 450 μL or 1.35 mL of the DMEM without FBS, respectively) was incubated with the cells for 1 h in a 24-well plate or confocal dish, and followed by incubation with fresh DMEM with 10% FBS for 1h unless otherwise mentioned. To study the colocalization with Hoescht 33342 or Lysotracker, the reagent was introduced 20 min before the observation.

CASP3 delivery

The procedure of CASP3 delivery was similar to that of GFP delivery, except that 30,000 HeLa cells were incubated in a 24-well plate for 24 h prior to delivery. After the protein delivery, the cells were stained by Yopro-1 and 7-AAD for 30 min, followed by the observation under fluorescence microscope. The apoptotic ratio of each sample was calculated as the ratio of fluorescently stained cells over total 100 cells.

Supplementary Material

Refer to Web version on PubMed Central for supplementary material.

Acknowledgments

This research was supported by the NIH (GM077173 and EB014277 to VMR and GM80532 to JAH). DJS acknowledges a NIH CBI training grant (S11110000000104). EMV acknowledges National Science Foundation training grants (S21000025700000 and DGE-0504485). The authors also appreciate D. Callaham for help with confocal imaging.

REFERENCES AND NOTES

1. Leader B, Baca QJ, Golan DE. Protein Therapeutics: A Summary and Pharmacological Classification. Nat. Rev. Drug Discov. 2008; 7:21–39. [PubMed: 18097458]
2. Yarden Y, Sliwkowski MX. Untangling the Erbb Signalling Network. Nat. Rev. Mol. Cell Biol. 2001; 2:127–137. [PubMed: 11252954]
3. Foltopoulou PF, Tsiftsoglou AS, Bonovolias ID, Ingendoh AT, Papadopoulou LC. Intracellular Delivery of Full Length Recombinant Human Mitochondrial L-Sco2 Protein into the Mitochondria of Permanent Cell Lines and Sco2 Deficient Patient's Primary Cells. Biochim. Biophys. Acta-Mol. Basis Dis. 2010; 1802:497–508.
4. Jo D, Liu DY, Yao S, Collins RD, Hawiger J. Intracellular Protein Therapy with Socs3 Inhibits Inflammation and Apoptosis. Nat. Med. 2005; 11:892–898. [PubMed: 16007096]
5. Beck M. Therapy for Lysosomal Storage Disorders. IUBMB Life. 2010; 62:33–40. [PubMed: 20014233]
6. Ogawa T, Ono S, Ichikawa T, Arimitsu S, Onoda K, Tokunaga K, Sugiu K, Tomizawa K, Matsui H, Date I. Protein Transduction Method for Cerebrovascular Disorders. Acta Med. Okayama. 2009; 63:1–7. [PubMed: 19247417]
7. Cai Z, Ye Z, Yang X, Chang Y, Wang H, Liu Y, Cao A. Encapsulated Enhanced Green Fluorescence Protein in Silica Nanoparticle for Cellular Imaging. Nanoscale. 2011; 3:1974–1976. [PubMed: 21369623]
8. Ma Y, Cai S, Lv Q, Jiang Q, Zhang Q, Sodmergen, Zhai Z, Zhang C. Lamin B Receptor Plays a Role in Stimulating Nuclear Envelope Production and Targeting Membrane Vesicles to Chromatin During Nuclear Envelope Assembly through Direct Interaction with Importin B. J. Cell Sci. 2007; 120:520–530. [PubMed: 17251381]
9. Shah DA, Kwon SJ, Bale SS, Banerjee A, Dordick JS, Kane RS. Regulation of Stem Cell Signaling by Nanoparticle-Mediated Intracellular Protein Delivery. Biomaterials. 2011; 32:3210–3219. [PubMed: 21296414]
10. Gaj T, Guo J, Kato Y, Sirk SJ, Barbas CF 3rd. Targeted Gene Knockout by Direct Delivery of Zinc-Finger Nuclease Proteins. Nat. Methods. 2012; 9:805–807. [PubMed: 22751204]
11. Patsch C, Kesseler D, Edenhofer F. Genetic Engineering of Mammalian Cells by Direct Delivery of Flp Recombinase Protein. Methods. 2011; 53:386–393. [PubMed: 21185381]
12. Zhou HY, Wu SL, Joo JY, Zhu SY, Han DW, Lin TX, Trauger S, Bien G, Yao S, Zhu Y, et al. Generation of Induced Pluripotent Stem Cells Using Recombinant Proteins. Cell Stem Cell. 2009; 4:581–581.
13. Zhang Y, Yu LC. Microinjection as a Tool of Mechanical Delivery. Curr. Opin. Biotechnol. 2008; 19:506–510. [PubMed: 18725294]
14. Lo SL, Wang S. Intracellular Protein Delivery Systems Formed by Noncovalent Bonding Interactions between Amphipathic Peptide Carriers and Protein Cargos. Macromol. Rapid Commun. 2010; 31:1134–1141. [PubMed: 21590866]
15. Gu Z, Biswas A, Zhao MX, Tang Y. Tailoring Nanocarriers for Intracellular Protein Delivery. Chem. Soc. Rev. 2011; 40:3638–3655. [PubMed: 21566806]
16. Foster S, Duvall CL, Crownover EF, Hoffman AS, Stayton PS. Intracellular Delivery of a Protein Antigen with an Endosomal-Releasing Polymer Enhances Cd8 T-Cell Production and Prophylactic Vaccine Efficacy. Bioconjugate Chem. 2010; 21:2205–2212.
17. Kaczmarczyk SJ, Sitaraman K, Young HA, Hughes SH, Chatterjee DK. Protein Delivery Using Engineered Virus-Like Particles. Proc. Natl. Acad. Sci. U. S. A. 2011; 108:16998–17003. [PubMed: 21949376]

18. Rudolph, GBR.; Lilie, H.; Jaenicke, R. Protein Function: A Practical Approach. Edn. 2. Creighton, TE., editor. Oxford; New York: 1997. p. 64
19. Bennion BJ, Daggett V. The Molecular Basis for the Chemical Denaturation of Proteins by Urea. Proc. Natl. Acad. Sci. U. S. A. 2003; 100:5142–5147. [PubMed: 12702764]
20. Melikov K, Chernomordik L. Arginine-Rich Cell Penetrating Peptides: From Endosomal Uptake to Nuclear Delivery. Cell. Mol. Life Sci. 2005; 62:2739–2749. [PubMed: 16231085]
21. Wadia JS, Stan RV, Dowdy SF. Transducible TAT-HA Fusogenic Peptide Enhances Escape of Tat-Fusion Proteins after Lipid Raft Macropinocytosis. Nat. Med. 2004; 10:310–315. [PubMed: 14770178]
22. Cronican JJ, Thompson DB, Beier KT, McNaughton BR, Cepko CL, Liu DR. Potent Delivery of Functional Proteins into Mammalian Cells *in vitro* and *in vivo* Using a Supercharged Protein. ACS Chem. Biol. 2010; 5:747–752. [PubMed: 20545362]
23. Salmaso S, Caliceti P. Self Assembling Nanocomposites for Protein Delivery: Supramolecular Interactions of Soluble Polymers with Protein Drugs. Int. J. Pharm. 2013; 440:111–123. [PubMed: 22209998]
24. Yang XC, Samanta B, Agasti SS, Jeong Y, Zhu ZJ, Rana S, Miranda OR, Rotello VM. Drug Delivery Using Nanoparticle-Stabilized Nanocapsules. Angew. Chem. Int. Ed. 2011; 50:477–481.
25. Doxsey SJ, Sambrook J, Helenius A, White J. An Efficient Method for Introducing Macromolecules into Living Cells. J. Cell Biol. 1985; 101:19–27. [PubMed: 2989298]
26. Almofti MR, Harashima H, Shinohara Y, Almofti A, Baba Y, Kiwada H. Cationic Liposome-Mediated Gene Delivery: Biophysical Study and Mechanism of Internalization. Arch. Biochem. Biophys. 2003; 410:246–253. [PubMed: 12573284]
27. Terlecky SR, Koepke JI. Drug Delivery to Peroxisomes: Employing Unique Trafficking Mechanisms to Target Protein Therapeutics. Adv. Drug Deliv. Rev. 2007; 59:739–747. [PubMed: 17659806]
28. Wiskur SL, Lavigne JL, Metzger A, Tobey SL, Lynch V, Anslyn EV. Thermodynamic Analysis of Receptors Based on Guanidinium/Boronic Acid Groups for the Complexation of Carboxylates, Alpha-Hydroxycarboxylates, and Diols: Driving Force for Binding and Cooperativity. Chem.-Eur. J. 2004; 10:3792–3804. [PubMed: 15281164]
29. Zafar A, Melendez R, Geib SJ, Hamilton AD. Hydrogen Bond Controlled Aggregation of Guanidinium-Carboxylate Derivatives in the Solid State. Tetrahedron. 2002; 58:683–690.
30. Ghosh P, Yang X, Arvizo R, Zhu ZJ, Agasti SS, Mo Z, Rotello VM. Intracellular Delivery of a Membrane-Impermeable Enzyme in Active Form Using Functionalized Gold Nanoparticles. J. Am. Chem. Soc. 2010; 132:2642–2645. [PubMed: 20131834]
31. Maruyama K. Intracellular Targeting Delivery of Liposomal Drugs to Solid Tumors Based on Epr Effects. Adv. Drug Deliv. Rev. 2011; 63:161–169. [PubMed: 20869415]
32. Jeong Y, Duncan B, Park MH, Kim C, Rotello VM. Reusable Biocatalytic Crosslinked Microparticles Self-Assembled from Enzyme-Nanoparticle Complexes. Chem. Commun. 2011; 47:12077–12079.
33. Yoshikawa T, Sugita T, Mukai Y, Abe Y, Nakagawa S, Kamada H, Tsunoda SI, Tsutsumi Y. The Augmentation of Intracellular Delivery of Peptide Therapeutics by Artificial Protein Transduction Domains. Biomaterials. 2009; 30:3318–3323. [PubMed: 19304319]
34. Zelphati O, Wang Y, Kitada S, Reed JC, Felgner PL, Corbeil J. Intracellular Delivery of Proteins with a New Lipid-Mediated Delivery System. J. Biol. Chem. 2001; 276:35103–35110. [PubMed: 11447231]
35. Cho KC, Jeong JH, Chung HJ, Joe CO, Kim SW, Park TG. Folate Receptor-Mediated Intracellular Delivery of Recombinant Caspase-3 for Inducing Apoptosis. J. Control. Release. 2005; 108:121–131. [PubMed: 16139916]
36. Zassler B, Blasig IE, Humpel C. Protein Delivery of Caspase-3 Induces Cell Death in Malignant C6 Glioma, Primary Astrocytes and Immortalized and Primary Brain Capillary Endothelial Cells. J. Neuro-Oncol. 2005; 71:127–134.
37. Lowe SW, Lin AW. Apoptosis in Cancer. Carcinogenesis. 2000; 21:485–495. [PubMed: 10688869]

38. Idziorek T, Estaquier J, De Bels F, Ameisen JC. Yopro-1 Permits Cytofluorometric Analysis of Programmed Cell Death (Apoptosis) without Interfering with Cell Viability. J. Immunol. Methods. 1995; 185:249–258. [PubMed: 7561136]

39. Zimmermann M, Meyer N. Annexin V/7-Aad Staining in Keratinocytes. Methods Mole. Biol. 2011; 740:57–63.

40. Richard JP, Melikov K, Vives E, Ramos C, Verbeure B, Gait MJ, Chernomordik LV, Lebleu B. Cell-Penetrating Peptides - a Reevaluation of the Mechanism of Cellular Uptake. J. Biol. Chem. 2003; 278:585–590. [PubMed: 12411431]

41. Carroll P, Schreuder LJ, Muwanguzi-Karugaba J, Wiles S, Robertson BD, Ripoll J, Ward TH, Bancroft GJ, Schaible UE, Parish T. Sensitive Detection of Gene Expression in Mycobacteria under Replicating and Non-Replicating Conditions Using Optimized Far-Red Reporters. PLoS One. 2010; 5:e9823. [PubMed: 20352111]

42. Dingwall C, Laskey RA. Protein Import into the Cell Nucleus. Annu. Rev. Cell Biol. 1986; 2:367–390. [PubMed: 3548772]

43. Henriques ST, Costa H, Castanho M. Translocation of Beta-Galactosidase Mediated by the Cell-Penetrating Peptide Pep-1 into Lipid Vesicles and Human Hela Cells Is Driven by Membrane Electrostatic Potential. Biochemistry. 2005; 44:10189–10198. [PubMed: 16042396]

44. Raagel H, Saalik P, Pooga M. Peptide-Mediated Protein Delivery-Which Pathways Are Penetrable? Biochim. Biophys. Acta-Biomembr. 2010; 1798:2240–2248.

45. Gould SJ, Keller GA, Hosken N, Wilkinson J, Subramani S. A Conserved Tripeptide Sorts Proteins to Peroxisomes. J. Cell Biol. 1989; 108:1657–1664. [PubMed: 2654139]

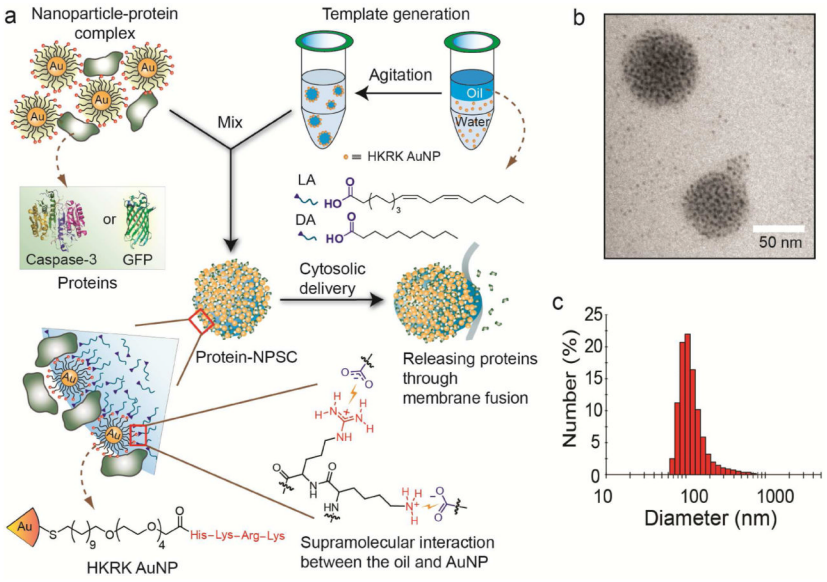

Figure 1.

Design and preparation of nanoparticle-stabilized capsules (NPSCs). (a) Schematic showing the preparation of the protein-NPSC complex containing caspase-3 or GFP and proposed delivery mechanism. The oil was a 1:1 mixture of linoleic acid (LA) and decanoic acid (DA). (b) TEM image of the dried GFP-NPSC. (c) Dynamic light scattering (DLS) histogram of GFP-NPSCs indicating an average diameter of 130 ± 40 nm.

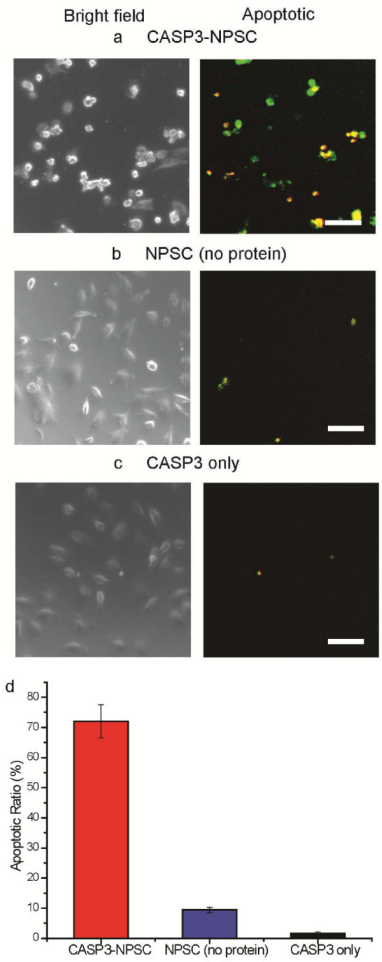

Figure 2.

Delivery of caspase-3 into HeLa cells. Cells were incubated for 1 h with (a) CASP3-NPSC, (b) NPSC without CASP3, and (c) only CASP3 without NPSC. Subsequently, cells were stained using Yopro-1 (green fluorescence) and 7-AAD (red fluorescence) for 30 min, and the overlapped images are presented as apoptotic. Individual channel images are shown in Figure S5. (d) Apoptosis ratios of the cells after CASP3 delivery. Scale bars: 100 μm; the error bars represent the standard deviations of three parallel measurements.

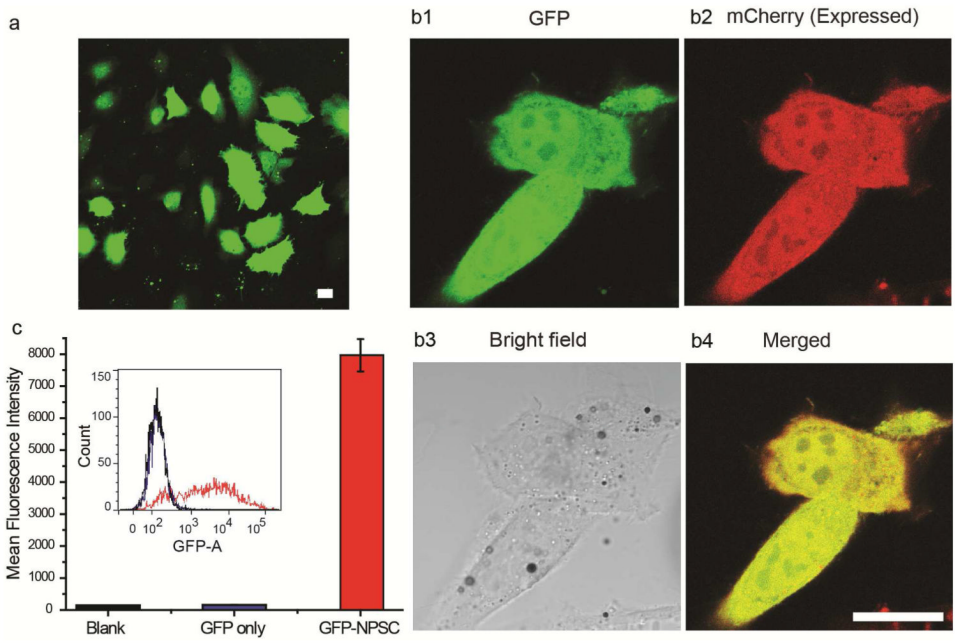

Figure 3.

Delivery of GFP into HeLa cells. (a) Confocal image showing GFP delivery into HeLa cells by NPSCs. (b) Confocal images showing the colocalization of delivered GFP with expressed mCherry in HeLa cell. (c) Flow cytometry results of HeLa cells treated with GFP-NPSCs (red), or GFP alone (blue) for 2 h, using untreated HeLa cells as the control (black). Scale bars: 20 μm.

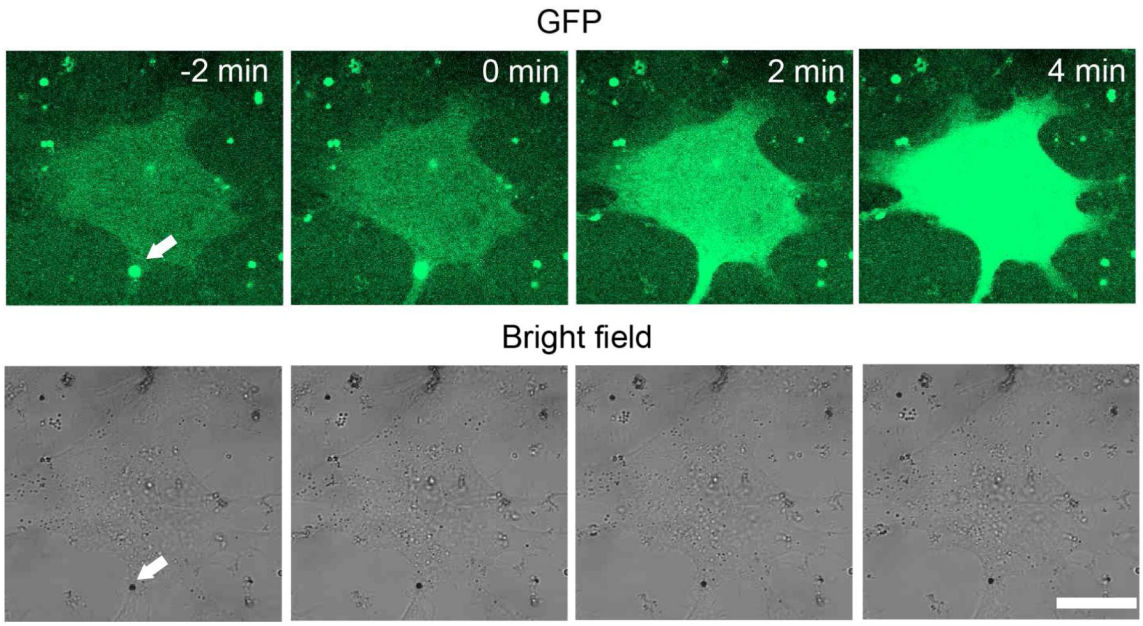

Figure 4.
Live cell imaging of rapid GFP release into the cytosol of HeLa cell by NPSCs. “0 min” label represents the starting point of release. The arrow indicates a GFP-NPSC at the cell membrane prior to delivery of payload. Scale bar: 20 μm.

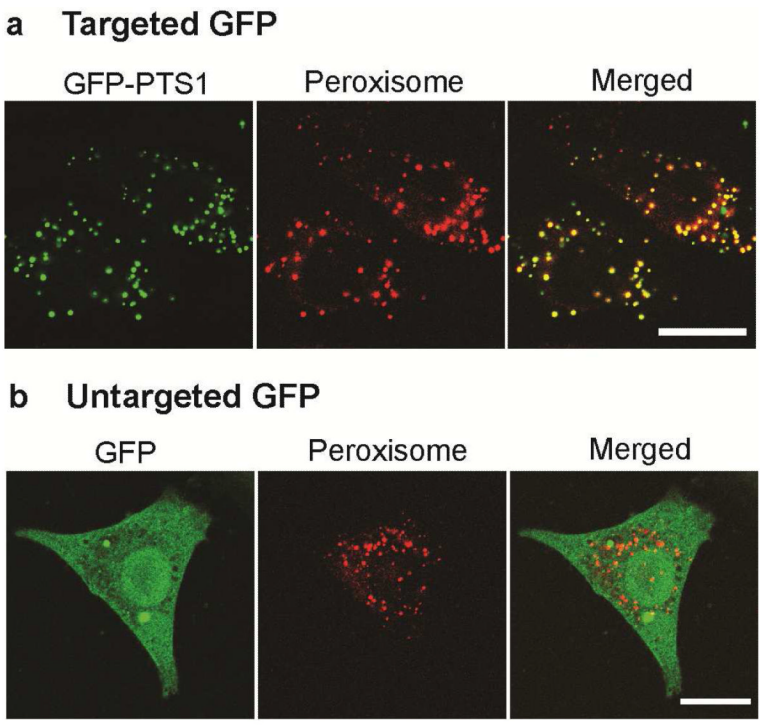

Figure 5.

Peroxisome targeting in HeLa cells transfected with RFP-PTS1 plasmid. (a) Colocalization of GFP-PTS1 fusion protein with the peroxisomal indicator (RFP-PTS1) expressed by the cell. (b) No colocalization of GFP was observed without PTS1 motif. Scale bars: 20 μm.